Available online at www.sciencedirect.com
SCIENCE DIRECT®
Journal of Catalysis 226 (2004) 410–421
JOURNAL OF CATALYSIS
www.elsevier.com/locate/jcat

An infrared study of the intermediates of methanol synthesis from carbon dioxide over Pd/β-Ga_2O_3

Sebastián E. Collins, Miguel A. Baltanás, Adrian L. Bonivardi *

Instituto de Desarrollo Tecnológico para la Industria Química (CONICET, UNL), Güemes 3450, 3000 Santa Fe, Argentina

Received 26 December 2003; revised 31 May 2004; accepted 5 June 2004

Available online 20 July 2004

Abstract

The interaction of CO_2 and H_2/CO_2 with pure β-Ga_2O_3 and Pd/β-Ga_2O_3 (1 wt% Pd) was studied by temperature-programmed reaction, between 323 K and 723 K at 0.1 MPa, using in situ FTIR spectroscopy. Under CO_2(g), bicarbonate, bidentate, and polydentate carbonate species are formed over the surface of gallia at 323 K. When β-Ga_2O_3 is exposed to H_2/CO_2 only polydentate carbonate reacts with hydrogen, at $T > 473$ K (i.e., after the dissociative adsorption of H_2 on gallia), to give bidentate and monodentate formate species (b-HCOO and m-HCOO, respectively) which are further hydrogenated to methoxy groups, just over 523 K. It is proposed that the addition of Pd to the oxide support only increases the hydrogenation rate of all the carbon-containing species bonded to the β-Ga_2O_3 surface, by spillover of atomic H from metallic Pd to gallia: (i) at 323 K (bi)carbonate groups are hydrogenated to m-HCOO and b-HCOO, and (ii) from 423 K upwards m-HCOO is further transformed to methoxy. A strong evidence of the interconversion between m-HCOO and b-HCOO was also found.

Keywords: Reaction intermediates; Methanol synthesis; Gallium oxide; Palladium catalyst; Carbon dioxide hydrogenation; Infrared spectroscopy; Gallium carbonate

1. Introduction

Recycling of carbon dioxide, the main manmade greenhouse gas, to give methanol via a catalytic hydrogenation process, has been lately under scrutiny as one of the strategies to decrease the concentration of atmospheric CO_2. In this regard, several catalysts have been proposed, e.g., Cu supported on metal oxides such as ZnO, ZrO_2, or Al_2O_3 [1–3]. As methanol synthesis is an exothermic reaction, the equilibrium conversion becomes smaller with increasing temperature. Therefore, efforts have been recently made toward the development of catalysts capable of operating at lower temperatures. In this context, supported precious metals, such as palladium, have shown interesting properties. Moreover, it has been shown that the support and the (eventual use of a) promoter can essentially modify both the activity and selectivity of Pd in methanol synthesis [4–6].

Among other novel candidates, gallium oxide has emerged as an exceptional material as a support [6,7] or promoter [8] in this reaction, causing deep changes on the catalytic properties of Pd for achieving effective conversion of carbon dioxide to methanol. The development of an active Pd/Ga_2O_3 catalyst for methanol synthesis from CO_2 hydrogenation, able to compete with the classical Cu/ZnO formulation, was first reported by Fujitani et al. [6]. Their Pd/Ga_2O_3 preparations showed the highest activity values for methanol production using H_2/CO_2 (3-to-1 mol ratio) at 5 MPa and were 120-fold more active than Pd on SiO_2 (an inert support) and 7-fold more active than Cu/ZnO/Al_2O_3 [6,7]. The other reaction product was CO (selectivity close to 49%), which was obtained via the reverse water gas shift reaction over the metallic palladium. Later on, Bonivardi et al. showed that addition of gallium nitrate to silica-supported Pd catalysts produced a dramatic en-

* Corresponding author. Fax: +54 342 4550944.
E-mail address: aboni@intec.unl.edu.ar (A.L. Bonivardi).

0021-9517/$ – see front matter
doi:10.1016/j.jcat.2004.06.012

hancement of the catalytic performance to give oxygenated compounds from carbon dioxide hydrogenation [8]: at 523 K and 3 MPa, the turnover rate to methanol improved up to 500-fold ($CO_2/H_2 = 1/3$) upon going from clean Pd/SiO_2 to $Ga\text{-}Pd/SiO_2$ with variable Ga-to-Pd atomic ratios (up to 8); the selectivity to methanol went up, from 17 to 70%, the higher the gallium content on the Pd/SiO_2 was.

Notwithstanding the effects of gallia over precious metals have been examined by various authors, there is no agreement regarding the means by which gallia promotes CO_2 reforming of methane or methanol synthesis from H_2/CO_2 mixtures. On one hand, Fujitani and co-workers postulated that the outstanding activity of Pd on gallia to the synthesis of methanol from carbon dioxide was due to an optimal amount of $Pd^{\delta+}$ ($0 < \delta < 2$) stabilized by GaO_x on the surface of palladium [6]. However, Inui concluded that the optimum of activity for the CO_2 reforming of methane on multifunctional catalysts on which gallium oxide and precious metals were incorporated could be controlled by a combination of direct and inverse hydrogen spillover from the noble metal and the gallium sites, respectively [9]. On the other hand, Bonivardi et al. [8] suggested that the mechanism of methanol synthesis from CO_2 hydrogenation on $Ga\text{-}Pd/SiO_2$ should involve intermediates from adsorbed CO_2 rather than CO, similar to those sustained by Cu/ZnO or over Cu/ZrO_2 [10–13]. Some of these intermediates were actually detected on Pd/Ga_2O_3 by Fujitani et al. at 523 K, using FTIR, but no exhaustive assignation of their IR signals and their evolutions was done [7].

Yet another aspect to consider is the ability of gallium oxide(s) to dissociate the hydrogen molecule on its own. Even though forms of reduced gallium, such as Ga(I) or GaH_x monomeric species, were proposed to play a crucial role in light alkane dehydrogenation and/or aromatization over supported-gallium catalysts [14–24], it is not straightforward to correlate gallium–hydrogen bond development with methanol synthesis from CO_2/H_2 mixtures on gallium–palladium/silica catalysts [25].

Thus, it seemed reasonable to us to focus on the activation processes of both molecular reactants, H_2 and CO_2, as well as on the surface species generated under reaction conditions on the surfaces of pure gallium oxide and supported palladium on gallia. Our results on the temperature-programmed reaction of H_2/CO_2 on well-defined $\beta\text{-}Ga_2O_3$ and $Pd/\beta\text{-}Ga_2O_3$ materials, followed by in situ infrared spectroscopy, are reported and discussed right after.

2. Experimental

2.1. Catalyst preparation and characterization

$\beta\text{-}Ga_2O_3$ support was obtained by calcination of commercial gallium (III) oxide (Strem Chemicals, 99.998 %Ga) at 1073 K for 4 h [26]. The crystallinity of the (single) beta phase was verified by XRD spectroscopy with a Shimadzu model XD-D1 diffractometer (Cu$K\alpha$ radiation).

In order to work with a well-defined polymorph of gallia (i.e., $\beta\text{-}Ga_2O_3$), and to prevent the loss of palladium into the Ga_2O_3 bulk, as it can occur when co-precipitation techniques are employed, we prepared a $Pd/\beta\text{-}Ga_2O_3$ catalyst by impregnation. Thus, a catalyst with 1 wt% Pd loading was prepared by incipient impregnation of the $\beta\text{-}Ga_2O_3$ with a solution of palladium (II) acetate (Sigma Chemical Co., 99.97%) in acetone. The "wet" precursor was air-dried in a mechanical convection oven at 343 K for 1 h to give $Pd(AcO)_2/\beta\text{-}Ga_2O_3$. This material was then calcined in flowing air (200 cm^3/min) in a glass reactor by heating from 298 to 673 K (2 h) at 2 K/min to obtain dispersed palladium oxide on the gallia surface. The $PdO/\beta\text{-}Ga_2O_3$ was reduced in a 5% v/v H_2/Ar mixture (200 cm^3/min), heating from 298 to 723 K (2 h) at 2 K/min. Before removing this reduced catalyst from the glass reactor, it was passivated at 298 K by flowing O_2/Ar mixtures (200 cm^3/min) with increasing O_2 content, from 0.1 to 5% v/v. For comparison purposes, the same treatment was also applied to the $\beta\text{-}Ga_2O_3$ support.

The specific surface area of the support and the catalyst were measured by the BET isotherm (N_2, 77 K) in a Micromeritics Accusorb 2000 unit. The fraction of exposed metallic palladium was determined by CO pulse chemisorption [27].

The catalytic performance for carbon dioxide hydrogenation was evaluated over both materials in a glass-lined SS microreactor for at least 24 h at 0.1 and 3 MPa (523 K, $H_2/CO_2 = 3/1$). The reaction products were analyzed by gas–liquid chromatography in two Shimadzu GC-9A units arranged in parallel (Carbosieve S-II 60/80 mesh and Porapack-QS 80/100 mesh, TCD and FID).

2.2. FT-IR studies

In situ transmission infrared spectroscopy was performed using 23 mg/cm^2 samples of each material (catalyst and support) pressed into self-supported wafers at 5 ton/cm^2. These wafers were located in turn in a Pyrex cell with water-cooled NaCl windows, which was attached to a conventional high-vacuum system (base pressure $= 1.33 \times 10^{-4}$ Pa), equipped with a manifold for gas flow, as described elsewhere [28]. The materials pretreatments and IR measurements were performed in situ at 0.1 MPa, except during evacuation. Before any experiments were performed, each sample was exposed to the following pretreatment procedure, to remove the artificial bands in the 3000–2800 cm^{-1} region which arise from oil contamination during wafers preparation and are attributed to C–H stretching modes [25]: first, O_2 was admitted into the cell (100 cm^3/min) and the temperature was raised from 298 to 723 K at 5 K/min and immediately lowered to 323 K under vacuum. Next, the cell was heated to 723 K at 5 K/min under H_2 (100 cm^3/min). After 30 min at this last condition the cell was evacuated for 20 min, still at 723 K. Finally, the temperature was gradually

decreased under vacuum to allow reference IR spectra of the "clean wafers" to be taken.

Temperature-programmed reaction experiments (TPR) were performed over the pretreated gallia and palladium/gallia, as follows: (i) pure CO_2 was flowed through the infrared cell (100 cm^3/min, 0.1 MPa) at 323 K for 30 minutes; (ii) H_2 was further added at this last temperature to the gas stream, adjusting the flows to the stoichiometric reactants ratio ($H_2/CO_2 = 3/1$, 140 cm^3/min, 0.1 MPa); (iii) the infrared cell was then heated to 723 K at 3 K/min (ascending ramp); and, last, (iv) temperature was decreased to 323 K (3 K/min) still flowing the reacting H_2/CO_2 mixture (descending ramp).

Infrared transmission spectra were acquired with a Shimadzu 8210 FT-IR spectrometer using a DLATGS detector (4 cm^{-1} resolution, 100 scans). Further processing of the spectra was carried out with the Microcal Origin 4.1 software. Background correction of the spectra was achieved by subtracting the spectra of the clean wafers at each temperature; a Lorentzian sum function was used for fitting the overlapped bands, measuring peak areas and/or intensities [29].

2.3. Gases

H_2 (AGA Ultra High Purity grade 99.999%) and CO_2 (Matheson, Coleman 99.99%) were further purified prior to use through a molecular sieve (3-Å Fisher) and MnO/Al_2O_3 traps, to remove water and oxygen impurities. O_2 (AGA Research grade 99.996%) was passed through a molecular sieve trap (3-Å Fisher) and Ascarite to remove water and carbon dioxide, respectively. D_2 (Scott C.P. grade 99.7%) was used without further purification.

3. Results and discussion

Table 1 summarizes the results of the catalytic performance of the gallia and palladium/gallia materials in the hydrogenation of CO_2 ($H_2/CO_2 = 3$; 523 K) after 24 h on stream.

Although β-Ga_2O_3 is not active for CO_2 hydrogenation, our Pd/β-Ga_2O_3 catalyst was about 130-fold more active at 3 MPa for methanol synthesis than a well-dispersed Pd/SiO_2 catalyst [8]. This remarkable enhancement of the catalytic activity towards methanol production is in agreement with the results previously reported by Fujitani et al. at similar experimental conditions [6]. Higher activity for CO production (via the RWGS reaction), close to 30-fold with respect to Pd/SiO_2, was also observed on palladium/gallia. Consequently, the Pd/β-Ga_2O_3 catalyst was 2.6-fold more selective for methanol production than Pd/SiO_2 at 3 MPa.

At low pressure (0.1 MPa), only the Pd/β-Ga_2O_3 catalyst was active for methanol production; within the analytical constraints of gas chromatography the equilibrium molar fraction of CH_3OH was reached, though.

Neither dimethylether nor methane was detected over the palladium-supported catalysts employing the H_2/CO_2 mixture, at any pressure. An additional experiment with a H_2/CO mixture (3/1) at 523 K and 0.1 MPa over the palladium/gallia catalyst did not show any activity to methanol, dimethylether or methane, either.

3.1. TPR of H_2/CO_2 on β-Ga_2O_3

The IR spectra between 323 and 723 K (ascending ramp), flowing H_2/CO_2 (3/1 mol ratio) over β-Ga_2O_3, are shown in Fig. 1. According to the various types of bands observed in the spectra, the whole temperature range can be split into two regions: a low-temperature region, from 323 to $\sim$ 473 K, and a high-temperature region, above $\sim$ 473 K.

The first spectrum shown in the low-temperature region was taken after flowing pure carbon dioxide for 30 minutes, at 323 K, over the sample of gallia. Clearly, these bands are a result of CO_2 chemisorption and are typical of carbonate species.

For the correct assignment of the signals (since to the best of our knowledge there are no IR spectra of gallium carbonates reported on the literature to be used as a fingerprint of these surfaces species chemisorbed onto β-Ga_2O_3), it is appropriate to examine the following features: (i) the thermal evolution of the intensity of each signal (thermal stability), (ii) the width of the ν_3-band splitting ($\Delta\nu_3 = \nu_{as} - \nu_s$, CO_3 stretching modes) of the CO_3^{2-} anion due to the loss of its D_{3h} symmetry by chemisorption [30,31], and (iii) the

Table 1
Catalytic performance of β-Ga_2O_3 and Pd/β-Ga_2O_3 for CO_2 hydrogenation under pseudo-steady-state conditions (after 24 h on stream)[a]

Material	FE[b] (%)	BET surface area (m^2/g)	P (MPa)	CO_2 conversion[c] (%)	Exit molar fraction (%)		Activity (10^{-3} mol Pd^{-1} s^{-1})		Selectivity (%)	
					CO[d]	CH_3OH[e]	CO	CH_3OH	CO	CH_3OH
β-Ga_2O_3	–	12	3	–	–	–	–	–	–	–
Pd/β-Ga_2O_3	31	12	3	0.86	0.104	0.113	69	75	48	52
			0.1	1.95	0.480	0.005	NA	NA	99	1

[a] $H_2/CO_2 = 3$, $T = 523$ K, SV = 82,000 h^{-1} (3 MPa), SV = 7700 h^{-1} (0.1 MPa).
[b] Initial percent fraction of exposed Pd (dispersion), measured by CO pulses [27].
[c] Total equilibrium conversion of CO_2, 22.0% (3 MPa), 16.6% (0.1 MPa).
[d] Equilibrium molar fraction of CO, 2.9% (3 MPa), 4.1% (0.1 MPa).
[e] Equilibrium molar fraction of CH_3OH, 2.9% (3 MPa), 0.005% (0.1 MPa).

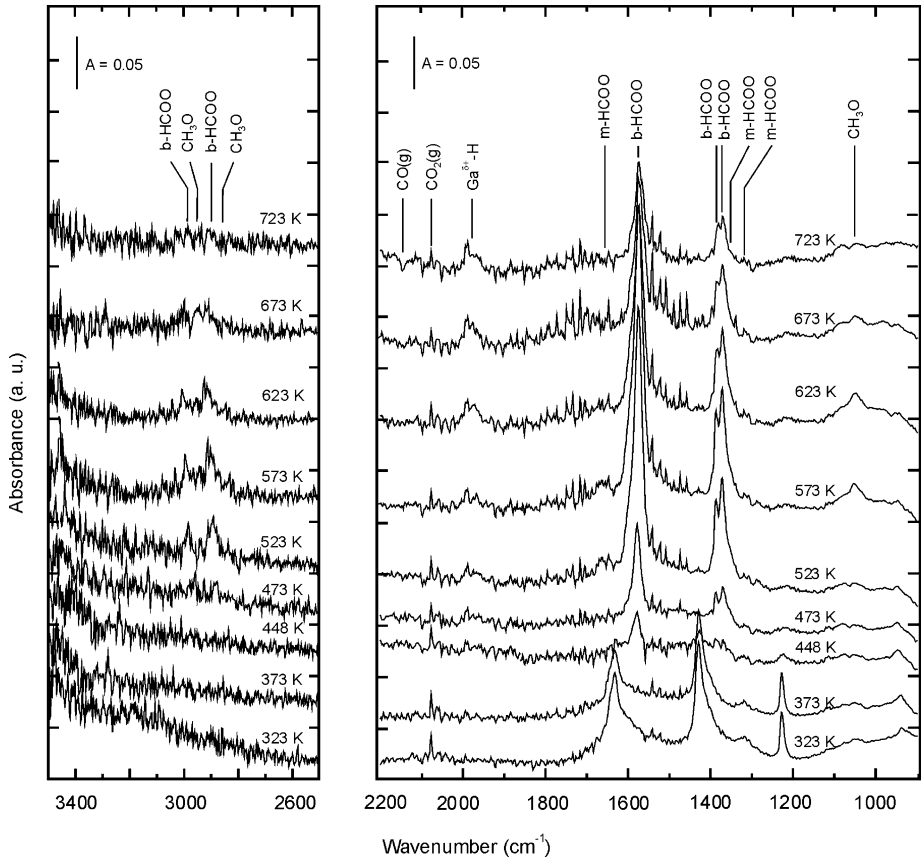

Fig. 1. Infrared spectra during the temperature-programmed reaction (TPR) of a $H_2/CO_2 = 3$ mixture flowing over prereduced β-Ga_2O_3 (140 cm^3/min) at 0.1 MPa (ascending ramp). The first spectrum (323 K) was taken after preexposing the sample to pure CO_2 for 30 min (100 cm^3/min).

wavenumber of the IR signals of carbonates adsorbed over other metal oxides.

The convoluted and resulting deconvoluted signals of the surface carbonates region, at 323 K, are shown in Fig. 2. The more intense bands, located at 1630, 1431, and 1225 cm^{-1}, are assigned to $\nu_{as}(CO_3)$, $\nu_s(CO_3)$, and δ(HO) modes, respectively, of a surface *bicarbonate* species (HCO_3^-) on gallium oxide. The ν_3-band splitting, 199 cm^{-1}, is identical to those of adsorbed bicarbonates (200 cm^{-1}) on different metal oxides [31–36]. Furthermore, the development of this group of bands was accompanied by the decaying of a broad band at ca. 3600 cm^{-1} assigned to the ν(OH) mode of interacting Ga–OH surface species. Thus, the formation of HCO_3^- is attributable to the reaction of CO_2 with hydroxyl groups present on the surface of gallia.

The signals located at 1587 and 1325 cm^{-1} in Fig. 2 are ascribed to the $\nu_{as}(CO_3)$ and $\nu_s(CO_3)$ modes of *bidentate carbonate* species (b-CO_3^{2-}). The band splitting for this surface species, $\Delta\nu_3 = 262$ cm^{-1}(close to the 300 cm^{-1} splitting found over other oxides) prevents its assignment to bridged carbonates, as the expected separation between the asymmetric and symmetric CO_3 stretching modes for the last type of carbonates is higher than 400 cm^{-1} [31–39].

Finally, two bands at ca. 1460 and 1406 cm^{-1} can also be distinguished on β-Ga_2O_3, which were highly overlapped at 323 K but became clearly visible when the other carbonate

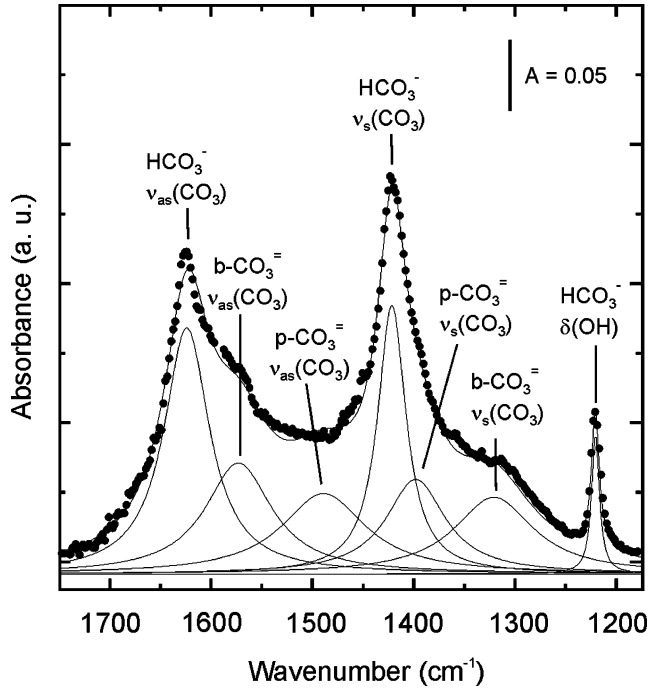

Fig. 2. Deconvoluted infrared signals for carbonates species on β-Ga_2O_3 during the adsorption of pure CO_2 (100 cm^3/min) at 0.1 MPa and 323 K.

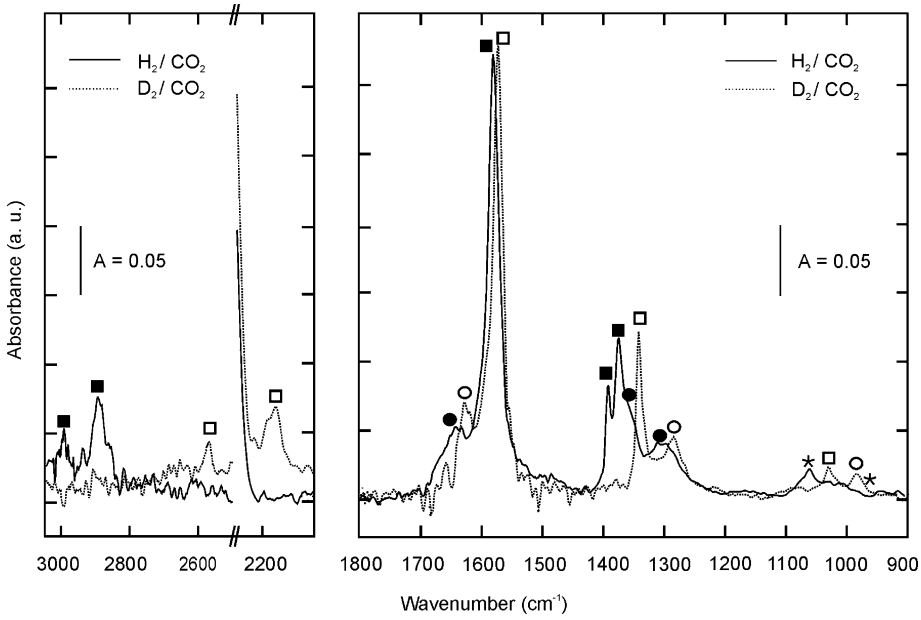

Fig. 3. Infrared spectra of bidentate (solid and open squares) and monodentate (solid and open circles) formates adsorbed over the surface of β-Ga_2O_3 at the end of both temperature-programmed reaction experiments (ascending and descending ramps). Experimental conditions: $H_2(D_2)/CO_2 = 3/1$, 0.1 MPa, 323 K (star: stretching mode of C–O for methoxy species).

signals faded out at about 473 K. These bands could account for the presence of either monodentate (m-CO_3^{2-}) or polydentate carbonate (p-CO_3^{2-}) species with commonly similar ν_3-band positions and $\Delta\nu_3 \leqslant 100$ cm^{-1} [31,32,35,37]. Yet, as regards the thermal stability of the different carbonate species, the surface m-CO_3^{2-} species should be expected to be much less stable than the p-CO_3^{2-} [31]. Because on this material all of the carbonate and bicarbonate signals immediately vanish after CO_2(g) evacuation (at 10^{-3} Pa) at room temperature, an extra experiment was run, flowing pure CO_2(g) and heating from 323 K to 723 K, holding constant the CO_2 pressure (0.1 MPa) at the same time. Only a tiny decrease of the intensity of the peaks at 1460 and 1406 cm^{-1} was observed upon increasing the temperature along this nonisothermal CO_2 adsorption experiment, although on heating both the b-CO_3^{2-} and HCO_3^- species decomposed. Therefore, these species, with strong thermal resistance and a rather low separation between the two C–O stretching modes should be thougth of as belonging to multiple bonded CO_2 over the gallium oxide surface, viz., *polydentate carbonate* species ($\nu_{as}(CO_3) = 1460$ cm^{-1} and $\nu_s(CO_3) = 1406$ cm^{-1}).

By rising the temperature above 453 K, several peaks emerged at 2991, 2898, 1640, 1580, 1386, 1372, 1350 (shoulder), and 1298 cm^{-1} (see Fig. 1). The wavenumbers corresponding to these bands suggest the presence of surface formates; alternatively, they might be ascribed to formyl species or CO_2 species bonded to surface cations [28,31,40–47].

To assign unambiguously these bands, we performed another TPR experiment, flowing a $D_2/CO_2 = 3$ mixture over β-Ga_2O_3, instead of H_2/CO_2. Fig. 3 shows the spectra at the end of both runs (ascending and descending temperature ramps—see below) with H_2/CO_2 and D_2/CO_2. First, it is clear that the whole set of signals shifted after isotopic substitution; then C is bonded to H(D) and, therefore, CO_2 complexes with the gallium cations are ruled out [31,40]. Second, no signal for the ν(CO) of surface formyl, usually around 1700 cm^{-1} [28,41–47], was detected. Hence, only formate species should account for those infrared peaks, i.e., monodentate and bidentate formate (from now on, m-HCOO and b-HCOO, respectively).

Both last species can be easily distinguished by the wavenumber location of their asymmetric and symmetric C–O stretching modes, as $\nu_{as}(CO_2)$ is higher for m-HCOO than for b-HCOO, while the opposite occurs for the position of the $\nu_s(CO_2)$ mode [31,37,39–41,48–69]. Additionally, Table 2 nicely shows that the assignments to all these bands to formates are unequivocal, in accordance with the near agreement between the experimental and predicted shifting of the band positions observed for their deuterated and hydrogenated forms. Nevertheless, the TPR experiments on gallia in the ramp of ascending temperature, unlike those on gallium oxide-supported palladium (vide infra), did not show a clear difference between the rate of formation of both types of formate, which reached their maximum surface concentration at ca. 550 K.

The appearance of another hydrogenated species from 523 K upwards, traceable to methoxy groups (CH_3O), was evident from the following additional infrared signals in the spectra: $\nu_s(CH) = 2942$ cm^{-1}, $\nu_{as}(CH) = 2831$ cm^{-1}, and $\nu(CO) = 1056$ cm^{-1} (Fig. 1) [28,41,67–74]. The highest concentration of methoxy on the surface of β-Ga_2O_3 oc-

Table 2
Observed infrared signals for bidentate and monodentate formate species over β-Ga_2O_3

Species	Vibration mode	ν_H[a] (cm^{-1}) HCOO	ν_D[b] (cm^{-1}) DCOO	ν_H/ν_D Experimental	ν_H/ν_D Calculated[c]
b-Formate	$\nu_{as}(CO_2)$	1580	1575	–	–
	δ(CH/D)	1386	1029	1.35	1.36
	$\nu_s(CO_2)$	1372	1342	–	–
	ν(CH/D)	2898	2176	1.33	1.36
	ν_1(comb)[d]	2991	2567	–	–
m-Formate	$\nu_{as}(CO_2)$	1640	1630	–	–
	δ(CH/D)	1350	986	1.37	1.36
	$\nu_s(CO_2)$	1298	1284	–	–

[a] Wavenumber for HCOO species.
[b] Wavenumber for DCOO species.
[c] $\nu_H/\nu_D = [\mu(CD)/\mu(CH)]^{1/2}$, where μ(CD) and μ(CH) are the reduced masses of CD and CH, respectively.
[d] Combination band, $\nu_1(comb) = \nu_{as}(CO_2) + \delta$(CH or CD).

curred at 600 K. Last, a weak feature due to CO in the gas phase (2150 cm^{-1}) was observed from 698 K as well.

In order to easily identify and summarize the location of the several IR bands recorded during the TPR experiments, a correlation chart is presented in Fig. 4. It was built by compiling the IR signals of some of the carbonaceous surface species usually found as intermediates of the methanol synthesis over several metal oxides or mixtures of metal oxides.

The TPR spectra, taken under the flowing H_2/CO_2 mixture over β-Ga_2O_3, neatly show that the surface concentration of bicarbonate and bidentate carbonate species decreased monotonically, to finally disappear at 473 K (see Fig. 5a). This behavior was identical to that one observed using just pure CO_2 (vide supra). Under the additional presence of H_2, however, the concentration of polydentate carbonate was constant until ca. 473 K, and this species was depleted only at higher temperature.

Concurrently, a band at about 1990 cm^{-1} emerged and, in the high temperature region ($T > 473$ K) the intensity of this peak increased, reaching a plateau at ca. 650 K (Figs. 1 and 5a). The FTIR spectra recorded during the in situ H_2 reduction pretreatment of the sample indicated that this last signal corresponded to the $Ga^{\delta+}$–H bond stretching vibration [25], except that it was about fourfold more intense with pure hydrogen. The origin of this 1990 cm^{-1} signal, which was previously reported by us on gallium(–palladium) silica-supported catalysts [25], was corroborated by a hydrogen–deuterium isotopic exchange experiment [$\nu(Ga^{\delta+}–D) = 1430$ cm^{-1}] on another sample of the gallium oxide.

Figs. 1 and 5a show that carbonate and bicarbonate species were formed at 323 K over the surface of clean gallium oxide under the flowing H_2/CO_2 reacting mixture and suggest, further, that the hydrogenation of the carbonaceus species, mostly polydentate carbonate, starts above 473 K (bicarbonate and bidentate carbonate are totally decomposed at this temperature), i.e., after the detection of the stretching mode of the $Ga^{\delta+}$–H bond. In other words, the hydrogenation of p-CO_3^{2-} proceeds right after the dissociative chemisorption of hydrogen molecule on partially reduced gallium sites sets in, giving formates and then methoxy species. Here, again, $Ga^{\delta+}$ cations seem to play an essential role in hydrogenation catalytic reactions, as in the

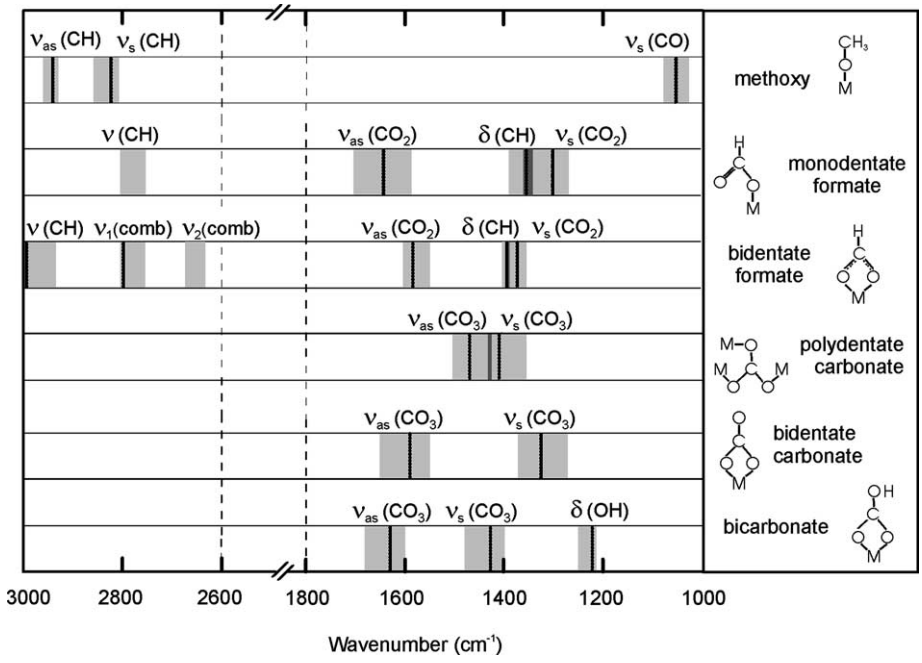

Fig. 4. Infrared vibrational frequency correlation chart of some of the carbonaceous surface species usually found as intermediates of the methanol synthesis over several metal oxides or mixtures of metal oxides [31–39,48–74]. The solid lines stand for the average of the wavenumber values measured in the present work. $\nu_1(comb) = \nu_{as}(CO_2) + \delta$(CH), and $\nu_2(comb) = \nu_s(CO_2) + \delta$(CH).

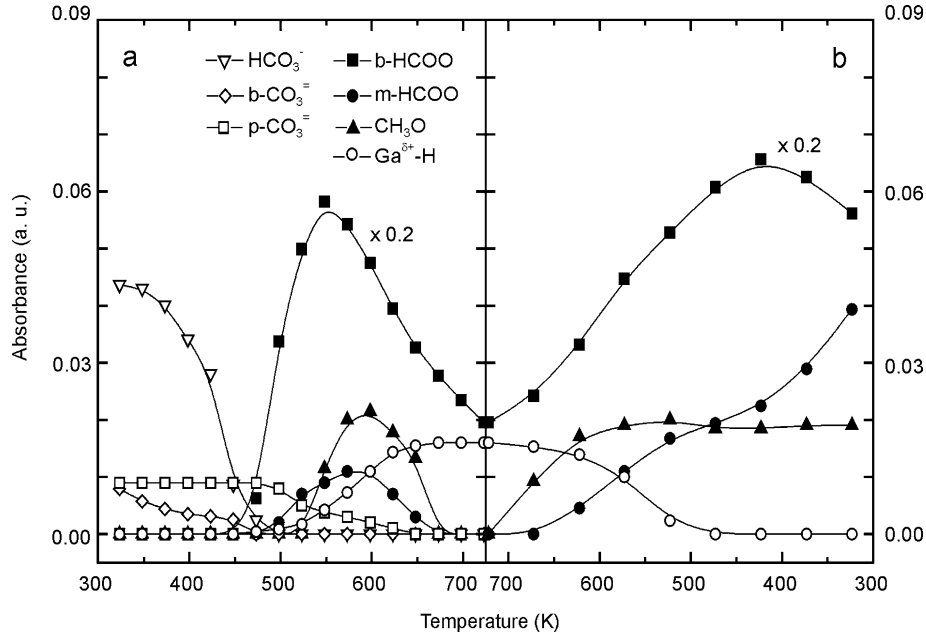

Fig. 5. Evolution of the intensity of the infrared bands of the surface species HCO_3^- [δ(OH) = 1225 cm^{-1}], b-CO_3^{2-} [$\nu_s(CO_3)$ = 1325 cm^{-1}], p-CO_3^{2-} [$\nu_{as}(CO_3)$ = 1460 cm^{-1}], b-HCOO [$\nu_{as}(CO_2)$ = 1585 cm^{-1}], m-HCOO [$\nu_{as}(CO_2)$ = 1640 cm^{-1}], CH_3O [ν(CO) = 1060 cm^{-1}], and $Ga^{\delta+}$–H [ν(Ga–H) = 1990 cm^{-1}], during the TPR over prereduced β-Ga_2O_3 using a $H_2/CO_2 = 3$ mixture (140 cm^3/min) at 0.1 MPa: (a) ascending and (b) descending temperature ramp.

case of propane dehydrogenation or dehydrocyclization over zeolite- and silica-supported gallium catalysts already mentioned [19–24].

Summing up, these data show that a (stepwise) hydrogenation of carbon dioxide takes place on β-Ga_2O_3, from polydentate carbonate to b-HCOO at first, which is further transformed into m-HCOO (onset at 523 K), being the last one hydrogenated to methoxy species thanks to the dissociative chemisorption of the hydrogen molecule over the oxide above 473 K.

Supplementary evidence of this last sequence can be collected from the evolution of the TPR infrared signals upon lowering the temperature, under the flowing H_2/CO_2 mixture (Fig. 5b). Although the coverage of the $Ga^{\delta+}$–H species decreased the lower the temperature was, the surface concentration of the hydrogenated carbonaceous species grew, but each signal increased in a different way. The concentration of methoxy groups evolved up to ca. 600 K and then remained essentially constant, with similar absorption intensity as the one reached at the maximum coverage of this species during the ramp of ascending temperature. Concurrently m-formates developed and kept accumulating over the oxide surface. Bidentate formates almost paralleled this increase up to ca. 473 K. Below this temperature, the surface coverage of b-HCOO started to level off, and then to decrease, while the production of m-HCOO went up. This last results can be rationalized as follows: at progressively lower temperature formate species accumulate over the surface, rather than react to give methoxy, whenever H_2 is no longer chemisorbed dissociatively over the gallium oxide, which happens below 473 K [25]. In the low-temperature range, monodentate formates still could be generated by interconversion from b-HCOO. Consequently, b-HCOO seems more stable than m-HCOO only at high temperature. We entirely disregard the hypothesis of CH_3O decomposition to give m-HCOO groups because the surface concentration of methoxy species is constant under 600 K.

However, neither carbonates nor bicarbonate species were regenerated at any temperature. This is an indication that the formate groups reside in the same Ga_2O_3 surface sites as (bi)carbonates species.

3.2. TPR of H_2/CO_2 on Pd/β-Ga_2O_3

Upon flowing pure CO_2 at 323 K for 30 min over Pd/β-Ga_2O_3, infrared bands ascribed to carbonates (poly and bidentate) and bicarbonate were readily observed (Fig. 6). The surface concentration of these species was similar to the one recorded over the clean oxide. Once H_2 was coadded into the flow of carbon dioxide, still at 323 K, the former species (HCO_3^-, b-CO_3^{2-} and p-CO_3^{2-}) rapidly vanished, and formates species bonded to the gallia surface arose instead. Fig. 6 displays that this isothermal conversion is fast enough to completely transform carbonates into formates in less than 3 min. Thereafter, no (bi)carbonates remained on the surface of the catalyst, while formates reached a constant concentration. Thus, the addition of Pd to β-Ga_2O_3 dramatically accelerates the formation of both formate species by hydrogenation of all (bi)carbonates as shown in Fig. 6, even at 323 K, unlike over the pure gallia where only p-CO_3^{2-} were hydrogenated ($T > 473$ K).

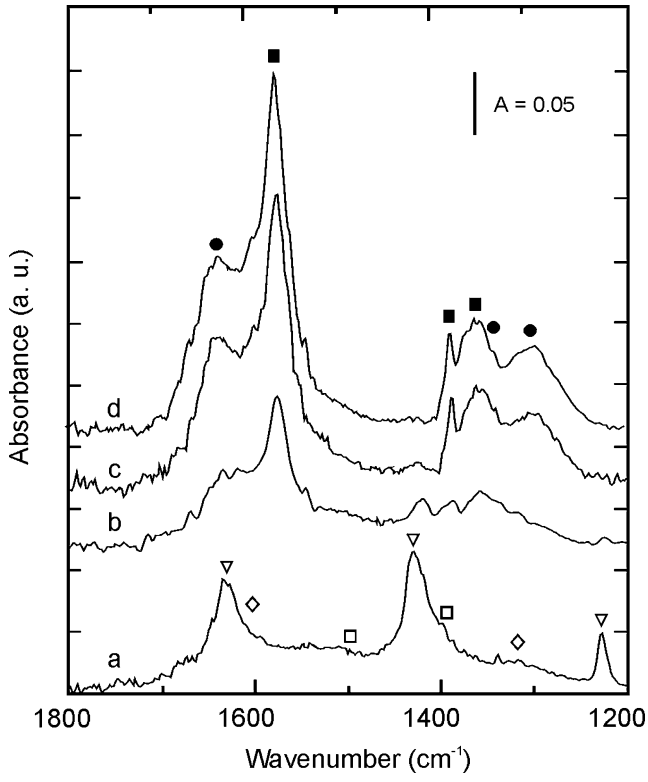

Fig. 6. Evolution of the infrared signals of surface carbonates and formates at 323 K over prereduced Pd/β-Ga_2O_3, after switching from a pure CO_2 stream (100 cm^3/min) to a $H_2/CO_2 = 3$ mixture (140 cm^3/min): (a) 0.0 min, (b) 1.5 min, (c) 2.0 min, and (d) 3.0 min. Total pressure = 0.1 MPa. (Symbols: as in Fig. 5.)

Fig. 7 shows the FTIR spectra coming from the TPR experiment (ascending ramp) under the $H_2/CO_2 = 3$ mixture over Pd/β-Ga_2O_3. The hydrogenated carbonaceous species detected are the same as those over the clean support. Nevertheless, the surface concentration and thermal evolution of some of them were remarkably different (compare Fig. 5a versus Fig. 8a). At increasing temperature m-formates were easily formed on gallia-supported palladium, coming up to a maximum value at 350 K and bidentate formate species, instead, reached the highest coverage at ca. 450 K. Almost concurrently with the depletion of monodentate formates, the C–O stretching band owing to methoxy groups could also be appreciated from 400 K onwards. Methoxy groups reached their maximum coverage at around 500 K.

The complete TPR data of Fig. 8 show, also, that m-HCOO is more reactive than b-HCOO, owing to the following: a careful inspection of the ascending ramp, between 350 K (after m-HCOO reaches its maximum surface concentration) and 400 K (before further hydrogenation takes place and methoxy is synthesized), neatly shows the mono–bidentate formate interconversion where, as was already pointed out, b-HCOO is more stable at high temperature. Furthermore, similarly to clean β-gallia m-HCOO is easier to hydrogenate than b-HCOO, which remains onto the gallia surface even at 723 K. Indeed, in Fig. 8a it can be appreciated that both the b-HCOO and m-HCOO bands lose intensity with almost parallel slopes but the latter does it at about 150 K higher temperature, what might well be interpreted as a stepwise transformation of b-HCOO into m-HCOO, and then methoxy (if b-HCOO were much more stable and difficult to hydrogenate).

Bands corresponding to chemisorbed CO (CO_s) revealed the presence of metallic palladium, as it was expected. A broad band under 2000 cm^{-1} and a peak at 2090 cm^{-1}) were already present at 323 K (see Fig. 7). They have been assigned to bridged and linear carbon monoxide (CO_B and CO_L, respectively) bonded to the surface of palladium [75–78]. On heating, the maximum of the low-frequency signal shifted from 1830 to 1970 cm^{-1} according to the changes in CO coverage. This broad signal is, actually, a convolution of several bands originated by various types of multicoordinated, bonded CO: dicoordinated CO on structurally open planes [Pd(210) or (100)] at approximately 1970 cm^{-1}, named B_1; dicoordinated CO on packed/compact planes [Pd(111)] close to 1956 cm^{-1}, named B_2; and triply bridging CO on Pd(111) below 1830 cm^{-1} assigned to CO seating in hollow sites (H band) [75]. No band could be detected for CO C-bonded to Pd with its oxygen atom bonded to a gallium cation, though. The vibration frequencies for this kind of surface complex usually lay below 1850 cm^{-1} [79–82].

Concerning the thermal evolution of these CO_s signals, both grew steadily, up to 400 K and 523 K, for CO_B and CO_L, respectively. With further temperature rising, the CO_s coverage went downward continuously and $CO_{(g)}$ was detected at $T > 543$ K (Fig. 8a). This is an indication of the occurrence of the reverse water gas shift (RWGS) reaction taking place over the surface of the palladium metal crystallites.

On cooling from 723 to 323 K, still keeping the flow of the H_2/CO_2 mixture, methoxy groups started to accumulate on the support from 600 K, i.e., 100 K less than on clean gallia. This has to be ascribed to the higher surface hydrogen concentration on the Pd/β-Ga_2O_3 than on pure β-Ga_2O_3. Then, the methoxy surface concentration leveled off under 423 K (Fig. 8b). This is approximately the same temperature at which methoxy was detected during the heating process. Seemingly, then, atomic hydrogen is available to form methoxy species until the reactivity of the partially hydrogenated carbonaceous intermediates (namely formates) is no longer able to yield CH_3O groups, at low temperature.

Fig. 8b also shows that the m-HCOO coverage in the descending temperature ramp followed the build-up curve of the ascending ramp almost as a mirror image. However, the inflection point at ca. 473 K could be an indication of the delayed formation of surface methoxy via another (undetected) hydrogenated intermediate: methylenebisoxy, which was observed by us on gallium–palladium silica-supported catalysts, most likely owing to their larger surface areas [83]. After that, the buildup of monodentate formate species under the cooling process resembled their growth under the heating ramp, i.e., when CH_3O groups ceased to be synthesized.

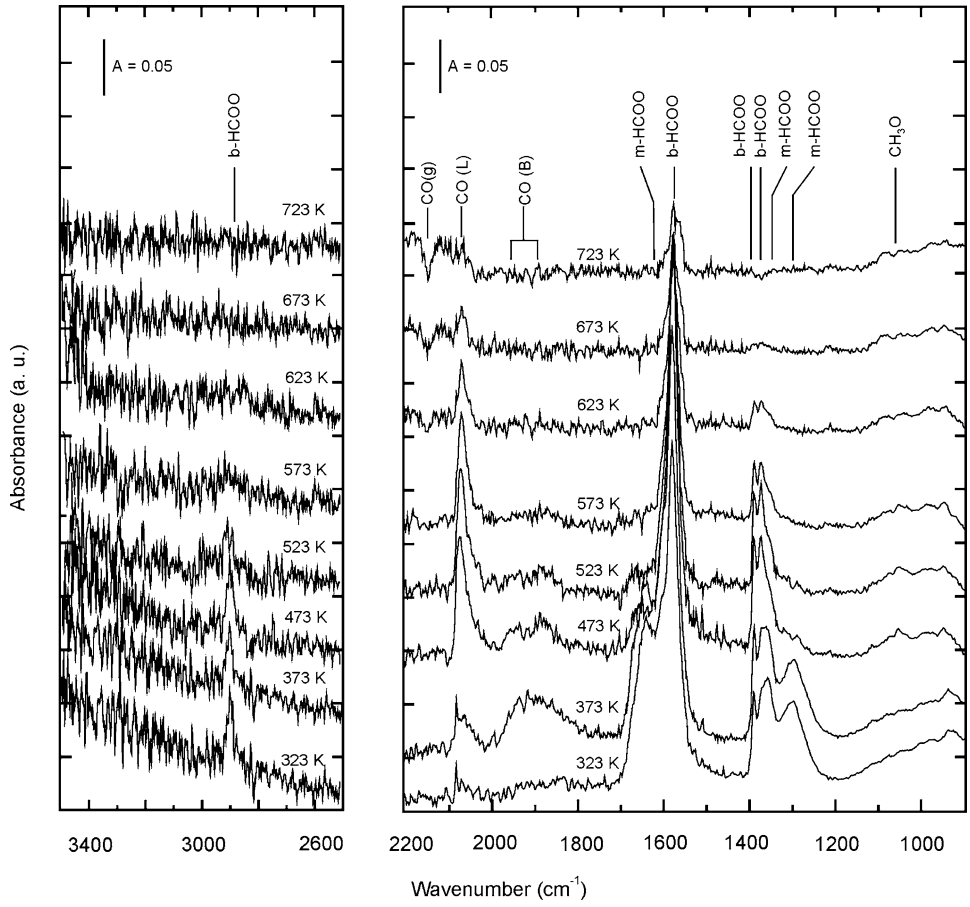

Fig. 7. Infrared spectra during the temperature-programmed reaction (TPR) over prereduced Pd/β-Ga_2O_3 of a $H_2/CO_2 = 3$ flowing mixture (140 cm^3/min) at 0.1 MPa (ascending ramp). The first spectrum (at 323 K) was taken after 3 min exposure to the reacting mixture (see Fig. 6d).

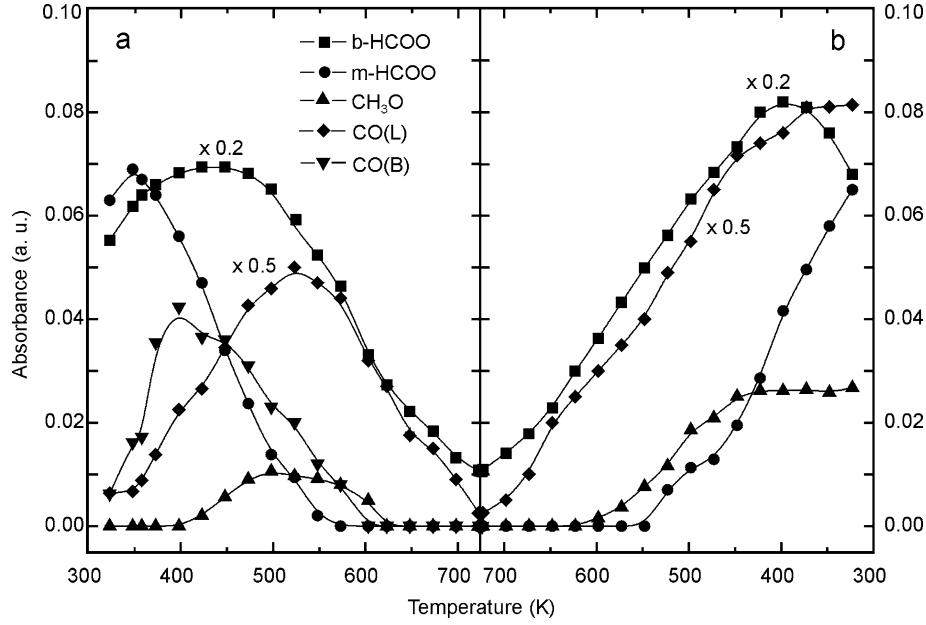

Fig. 8. Evolution of the intensity of the infrared bands of the surface species b-HCOO [$\nu_{as}(CO_2) = 1585$ cm^{-1}], m-HCOO [$\nu_{as}(CO_2) = 1640$ cm^{-1}], CH_3O [$\nu(CO) = 1060$ cm^{-1}], CO (B: bridged) [$\nu(CO) \sim 1900$ cm^{-1}], and CO (L: linear) [$\nu(CO) = 2090$ cm^{-1}] during the TPR over prereduced Pd/β-Ga_2O_3 using an $H_2/CO_2 = 3$ mixture (140 cm^3/min) at 0.1 MPa: (a) ascending and (b) descending temperature ramp. For clarity, the $\nu(Ga^{\delta+}$–H) (1990 cm^{-1}) band was not included.

Additionally, CO_s steadily accumulated over the Pd crystallites, to reach full coverage on decreasing the temperature up to 400 K, thus blocking the dissociative chemisorption of H_2 on the palladium metal, from approximately the same last temperature [84]. Surprisingly, CO_B was not detected in the ramp of descending temperature.

The concentration of b-HCOO on the gallia surface grew steadily, till 400 K. With further cooling bidentate formate began to decompose, but the build up of m-HCOO on the surface still went on. Since b-HCOO decomposes under 423 K and no (bi)carbonates are present, it is verified, once more, that the transformation or interconversion of b-HCOO into m-HCOO suffices to explain these changes in their surface concentration, like on β-Ga_2O_3.

As indicated above, palladium metal on the surface (and as a consequence, atomic hydrogen supply) fastens every hydrogenation step: the onset of methoxy formation was 400 K vs 523 K on palladium–gallia and clean gallia, respectively (Figs. 5a and 8a). Yet, even with enough atomic hydrogen supply (Pd/β-Ga_2O_3 catalyst), the rate for the reaction step(s) of m-HCOO reduction to give CH_3O was faster under 500 K than the release of methoxy species from the catalyst surface (compare the concentration of all these species in Fig. 8a).

Regardless: (i) the maximum surface concentration of CH_3O on gallia was twice that on palladium–gallia, and (ii) this maximum and the offset of the methoxy signals are downshifted by about 100 K in the metal-oxide catalyst as compared to the clean support. These last two observations are congruent with reductive, rather than hydrolytic, elimination of the methoxy species from Ga_2O_3. Further work is in progress to clarify this point [83].

For a low amount of available atomic surface hydrogen, like in the case of β-Ga_2O_3 under (or at) 523 K, the overall rate for the hydrogenation reaction of the carbonaceous species is so low that neither methoxy showed up on the TPR experiments in the (0.1 MPa) infrared cell (Fig. 5a) nor methanol gas was produced in the activity test experiments performed at 3 MPa in the flow microreactor (Table 1).

To certify that gaseous methanol was produced in the infrared reaction cell using a Pd/β-Ga_2O_3 wafer, another identical cell (detection cell) was connected on line at the exhaust of the previous one. A silicagel wafer (SiO_2 Davison Grade 29, 10 mg/cm^2) was placed into the detection cell, dried in situ and kept at 393 K while operating the reaction cell with a $H_2/CO_2 = 3$ mixture at 523 K and 0.1 MPa. After 30 min of reaction, the infrared peaks at 2858 and 2960 cm^{-1} [ν_s (CH_3) and ν_{as} (CH_3), respectively], characteristic of sorbed methanol over SiO_2 were detected [28]. Another point of concern refers to the role of the Pd–gallia interface. One could be tempted to think that the formation of formate species is confined to this interface and that, then, those formates migrate over the whole gallia surface. Yet, upon comparing the intensity of the formates bands over gallia vs Pd/gallia, it is difficult to sustain that the reaction on the last material is circumscribed to the Pd–gallia interface: the surface concentration of m-fomate is lower on clean gallia than on Pd/gallia and, even though the amount of b-formate was almost the same in both systems, the temperature of formation of both species was considerably different for each material (Figs. 5a and 8a). Furthermore, TPR-FTIR over a *mechanical mixture* of Pd/SiO_2 + Ga_2O_3/SiO_2, where the only contact point are those of the silica support particles, showed formates formation at 125 K less than on Ga_2O_3/SiO_2 alone and with higher surface concentration (we kept the gallium loading constant). Complementarily, we also run reaction experiments with mechanical mixtures of Pd/SiO_2 + Ga_2O_3/SiO_2 (at 3 MPa) where aliquots of each material were combined in different proportions and a "volcano-type" curve for the methanol production was obtained [85]. Thus, we strongly believe that, on Pd/β-Ga_2O_3 catalyst, atomic hydrogen spills over and migrates over the gallia surface, rather than formate formation at and migration from the palladium–gallia interface.

Scheme 1 summarizes the proposed reaction pathway for the methanol synthesis from carbon dioxide and hydrogen over our palladium/gallia catalyst. So, gaseous CO_2 is weakly adsorbed over the gallia surface, giving carbonate and bicarbonate groups. These (bi)carbonates react with atomic hydrogen, which is supplied by spillover from the Pd crystallites, producing mono- and bidentate formates, which

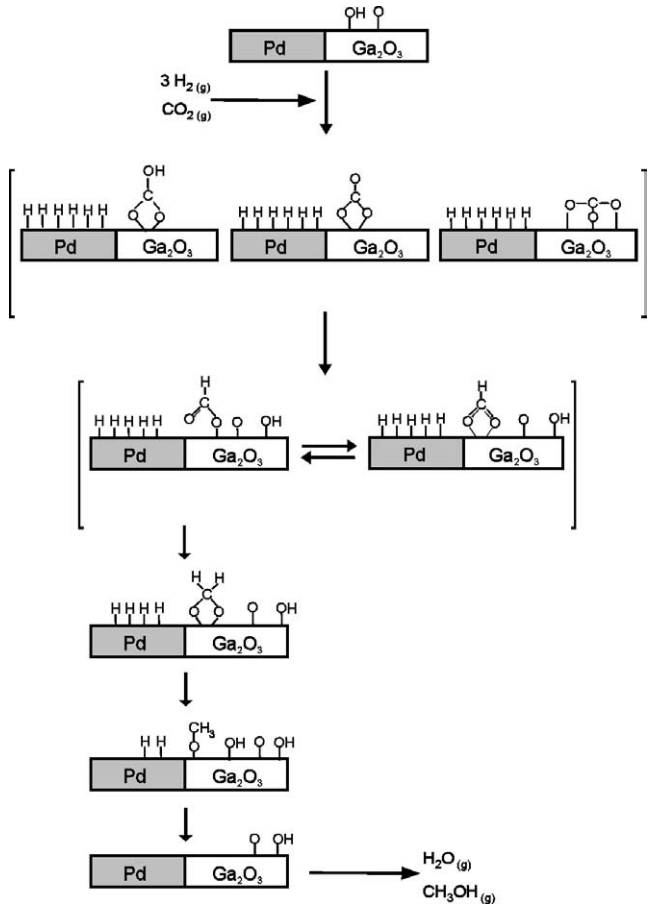

Scheme 1.

can interconvert on the surface. The m-HCOO formed is further hydrogenated (probably to methylenebisoxy groups and then) to methoxy species.

Methylenebisoxy species (H_2COO) was not detected over the pure support or the Pd/Ga_2O_3 catalyst. However, its formation was observed on Ga_2O_3/SiO_2 and Ga_2O_3–Pd/SiO_2 under identical reaction conditions [83]. We think that the stability of methylenebisoxy groups may be intrinsically related to the oxide over which they are adsorbed, and that silica offers a better stability for this intermediate than gallium oxide does. In this respect, the product molecule (methoxy) is much more stable on SiO_2 [28] than is on gallia.

Be that as it may, even though m-HCOO hydrogenation seems the most likely route to form methoxy species and that b-HCOO, owing to its accumulation on the surface, is inferred to be more stable and hard to hydrogenate, we cannot entirely rule out the b-HCOO hydrogenation route to methanol by just analyzing our data.

Finally, an efficient spillover of atomic hydrogen from the palladium crystallites to the carbonaceous species chemisorbed over the gallium oxide, combined with a moderate stability of the methoxy species on the gallia surface, seem to be the most plausible explanation for the outstanding activity and selectivity of the palladium-gallium system.

4. Conclusions

β-Ga_2O_3 is able to (weakly) chemisorb carbon dioxide at room temperature, as bicarbonate and carbonate (bi- and polydentate) surface species. Bicarbonates are formed by reaction between the CO_2 molecules with Ga–OH from the surface and, like bidentate carbonates, are totally decomposed under flowing CO_2 at temperatures higher than 473 K. Polydentate carbonates are more stable, and are hydrogenated (under the reactive H_2/CO_2 mixture) to bidentate formate species at $T > 473$ K, when H_2 can be dissociatively chemisorbed by gallium cations (giving $Ga^{\delta+}$–H moieties). Bidentate formates are further converted, stepwise, to monodentate formates and finally to methoxy groups.

After the addition of palladium to β-gallia, these processes are greatly accelerated, rather than modified. As Pd is able to dissociate hydrogen molecules even at subambient temperature, all (bi)carbonates bonded to gallia are hydrogenated to monodentate and bidentate formate species by hydrogen atoms spiltover from the metal crystallites even at 323 K, the lowest temperature used in this work. Then, the picture remains as in the case of pure gallia: when the temperature increases those formates are hydrogenated to methoxy species. Finally, a reductive rather than a hydrolytic elimination of methoxy groups closes the catalytic sequence over the surface of the Pd/gallia catalyst.

There is strong experimental evidence of interconversion between b- and m-formate, showing that this is an exothermic, reversible reaction. But, even so, since b-formates prevail over the surface of gallia for both type of materials (pure gallia or palladium/gallia) even at 723 K, it seems that m-HCOO is actually the most reactive intermediate of the process.

A sequence for the methanol synthesis from carbon dioxide is proposed to explain the catalytic properties of the Pd-Ga system and to understand which are the key steps in the hydrogenation of carbon oxides on it.

Acknowledgments

This work was supported by the Consejo Nacional de Investigaciones Científicas y Técnicas (CONICET) and the Agencia Nacional para la Promoción de la Ciencia y la Tecnología (ANPCyT) of Argentina.

References

[1] S. Fujita, M. Usui, H. Ito, N. Takezawa, J. Catal. 157 (1995) 403.
[2] T.C. Schilke, I.A. Fisher, A.T. Bell, Catal. Lett. 54 (1998) 105.
[3] I.A. Fisher, H.C. Woo, A.T. Bell, Catal. Lett. 44 (1997) 11.
[4] W.X. Pan, R. Cao, D.L. Roberts, G.L. Griffin, J. Catal. 114 (1988) 440.
[5] G.C. Chinchen, K.C. Waugh, D.A. Wham, Appl. Catal. 25 (1986) 101.
[6] T. Fujitani, M. Saito, Y. Kanai, T. Watanabe, J. Nakamura, T. Uchijima, Appl. Catal. A 125 (1995) L199.
[7] T. Fujitani, I. Nakamura, Bull. Chem. Soc. Jpn. 75 (2002) 1393.
[8] A.L. Bonivardi, D.L. Chiavassa, C.A. Querini, M.A. Baltanás, Stud. Surf. Sci. Catal. D 130 (2000) 3747.
[9] T. Inui, Catal. Today 29 (1996) 329.
[10] I.A. Fisher, A.T. Bell, J. Catal. 172 (1997) 222.
[11] I.A. Fisher, A.T. Bell, J. Catal. 178 (1998) 153.
[12] T.C. Schilke, I.A. Fisher, A.T. Bell, J. Catal. 184 (1999) 144.
[13] K.-D. Jung, A.T. Bell, J. Catal. 193 (2000) 207.
[14] G.L. Price, V. Kanazirev, J. Catal. 126 (1990) 267.
[15] G. Buckles, J. Hutchings, C.D. Williams, Catal. Lett. 8 (1991) 115.
[16] G. Buckles, J. Hutchings, Catal. Lett. 27 (1994) 361.
[17] M. Barre, N.S. Gnep, P. Magnoux, S. Sansare, V.R. Choudhary, M. Guisnet, Catal. Lett. 21 (1993) 275.
[18] G.D. Meitzner, E. Iglesia, J.E. Baumgartner, E.S. Huang, J. Catal. 140 (1993) 209.
[19] J.R. Mowry, R.F. Anderson, J.A. Johnson, Oil Gas J. 83 (1985) 1288.
[20] H. Kitagawa, Y. Sendoda, T. Ono, J. Catal. 101 (1986) 12.
[21] L.M. Thomas, X. Liu, J. Phys. Chem. 90 (1986) 4843.
[22] N.S. Gnep, J.Y. Doyenet, A.M. Seco, F. Ramoa Ribeiro, M. Guisnet, Appl. Catal. 43 (1988) 105.
[23] N.S. Gnep, J.Y. Doyenet, M. Guisnet, J. Mol. Catal. 45 (1988) 281.
[24] N.S. Nesterenko, O.A. Ponomoreva, V.V. Yuschenko, I.I. Ivanova, F. Testa, F. Di Renzo, F. Fajula, Appl. Catal., in press.
[25] S.E. Collins, M.A. Baltanás, J.L. Garcia Fierro, A.L. Bonivardi, J. Catal. 211 (2002) 252.
[26] K. Nishi, K. Shimizu, M. Takamatsu, H. Yoshida, A. Satsuma, T. Tanaka, S. Yoshida, T. Hattori, J. Phys. Chem. B 102 (1998) 10190.
[27] C.S. Fung, C.A. Querini, J. Catal. 138 (1992) 240.
[28] G.C. Cabilla, A.L. Bonivardi, M.A. Baltanás, J. Catal. 201 (2001) 213.
[29] J.D. Ingle Jr., S.R. Crouch, in: Spectrochem. Anal., first ed., Prentice–Hall, Upper Saddle River, NJ, 1988, p. 211.
[30] K. Nakamoto, J. Fujita, S. Tanaka, M. Kobayashi, J. Am. Chem. Soc. 79 (1958) 3197.
[31] G. Busca, V. Lorenzelli, Mater. Chem. 7 (1982) 89, and references therein.
[32] B. Bachiller-Baeza, I. Rodriguez-Ramos, A. Guerrero-Ruiz, Langmuir 14 (1998) 3556.

[33] J.V. Evans, T.L. Whateley, Trans. Faraday Soc. 63 (1967) 2769.
[34] A.A. Davydov, M.L. Shepotko, A.A. Budneva, Kinet. Katal. 35 (1994) 272.
[35] K. Pokrovski, K.T. Jung, A.T. Bell, Langmuir 17 (2001) 4297.
[36] R. Philipp, K. Fujimoto, J. Phys. Chem. 96 (1992) 9035.
[37] Q. Sun, C. Liu, W. Pan, Q. Zhu, J.F. Deng, Appl. Catal. A 171 (1998) 301.
[38] F. Ouyang, K. Nakayama, K. Tabarda, E. Suzuki, J. Phys. Chem. B 104 (2000) 2012.
[39] A.A. Davydov, V.G. Mikhaltchenko, V.D. Sokolvskii, G.K. Boreskov, J. Catal. 55 (1978) 299.
[40] D.H. Gibson, Coord. Chem. Rev. 185–186 (1999) 335, and references therein.
[41] L.Z. Gao, C.T. Au, J. Catal. 189 (2000) 1.
[42] D. Bianchi, T. Chafik, M. Khalfallah, S.J. Teichner, Appl. Catal. A 105 (1993) 223.
[43] C. Xu, D.W. Goodman, J. Phys. Chem. 100 (1996) 245.
[44] R. Burch, S. Chalker, J. Pritchard, J. Chem. Soc. Faraday Trans. 87 (1991) 193.
[45] H. Yang, J.L. Whitten, Langmuir 11 (1995) 853.
[46] D. Demri, L. Chateau, J.P. Hindermann, A. Kiennemann, M.M. Bettahar, J. Mol. Catal. A 104 (1996) 237.
[47] J. Saussey, J.C. Lavalley, J. Lamotte, T. Rais, J. Chem. Soc. Chem. Commun. (1982) 278.
[48] D.B. Clarke, A.T. Bell, J. Catal. 154 (1995) 314.
[49] A. Bandara, J. Kubota, A. Wada, K. Domen, C. Hirose, J. Phys. Chem. B 101 (1997) 361.
[50] F. Le Peltier, P. Chaumette, J. Saussey, M.M. Bettahar, J.C. Lavalley, J. Mol. Catal. A 122 (1997) 131.
[51] F. Le Peltier, P. Chaumette, J. Saussey, M.M. Bettahar, J.C. Lavalley, J. Mol. Catal. A 132 (1998) 91.
[52] J.C. Saussey, J.C. Lavalley, J. Mol. Catal. A 50 (1989) 343.
[53] G. Millar, C. Rochester, K.C. Waugh, J. Chem. Soc. Faraday Trans. 87 (1991) 1491.
[54] G. Millar, C. Rochester, K.C. Waugh, J. Chem. Soc. Faraday Trans. 87 (1998) 2785.
[55] G. Millar, C. Rochester, K.C. Waugh, J. Catal. 155 (1995) 52.
[56] M.M. Mohamed, M. Ichikawa, J. Colloid Interface Sci. 232 (2000) 381.
[57] K.K. Bando, K. Sayama, H. Kusama, K. Okabe, H. Arakawa, Appl. Catal. A 165 (1997) 391.
[58] F. Ouyang, A. Nakamara, K. Tabada, E. Suzuki, J. Phys. Chem. B 104 (2000) 2010.
[59] M. Haneda, N. Bio, M. Daturi, J. Saussey, J.C. Lavalley, D. Duprez, H. Hamada, J. Catal. 206 (2002) 114.
[60] E. Guglielminotti, E. Giamello, F. Pinna, G. Strukul, S. Martinengo, L. Zanderighi, J. Catal. 146 (1994) 422.
[61] V. Boiadjiev, W.T. Tysoe, Chem. Mater. 10 (1998) 334.
[62] I. Nakamura, H. Nakato, T. Fujitani, T. Uchijima, J. Nakamura, Surf. Sci. 402–404 (1998) 92.
[63] Z. Zhang, A. Kladi, E. Verykios, J. Catal. 156 (1995) 37.
[64] M. Hara, M. Kawamura, J. Kondo, K. Domen, K. Manuya, J. Phys. Chem. 100 (1996) 14462.
[65] G. Busca, J. Lamotte, J.C. Lavalley, V. Lorenzelli, J. Am. Chem. Soc. 109 (1987) 5197.
[66] X. Mugniery, T. Chafik, M. Primet, D. Bianchi, Catal. Today 52 (1999) 15.
[67] J. Weigel, R.A. Koeppel, A. Baiker, A. Wokaun, Langmuir 12 (1996) 5319.
[68] A.M. Efstathiou, T. Chafik, D. Bianchi, C.O. Bennett, J. Catal. 148 (1994) 224.
[69] C. Li, K. Domen, K. Maruya, T. Onishi, J. Catal. 141 (1993) 540.
[70] L.J. Burcham, L.E. Briand, I.E. Wachs, Langmuir 17 (2001) 6164.
[71] J.D. Odom, F.M. Wafacz, J.F. Sullivan, J.R. Durig, J. Raman Spectrosc. 11 (1981) 469.
[72] K. Mudalige, M. Trenary, J. Phys. Chem. B 105 (2001) 3823.
[73] M. Valet, D.M. Hoffmann, Chem. Mater. 13 (2001) 2135.
[74] D.B. Clarke, D. Lee, M.J. Sandoval, A.T. Bell, J. Catal. 150 (1994) 81.
[75] G.C. Cabilla, A.L. Bonivardi, M.A. Baltanás, Catal. Lett. 55 (1998) 147.
[76] R.F. Hicks, A.T. Bell, J. Catal. 90 (1984) 205, and references therein.
[77] F.M. Hoffmann, Surf. Sci. Rep. 3 (1983) 1.
[78] R.P. Eischens, W.A. Pliskin, Adv. Catal. 10 (1958) 1.
[79] G.C. Cabilla, A.L. Bonivardi, M.A. Baltanás, Appl. Catal. A Gen. 255 (2003) 181.
[80] S.S. Buojana, D. Demri, A. Cresselly, A. Hiennemann, J.P. Hindermann, Catal. Lett. 7 (1990) 359.
[81] V. Pitchon, M. Primet, H. Praliaud, Appl. Catal. 62 (1990) 317.
[82] A. Bonivardi, C. Pistonesi, M. Menghini, A. Juan, Comput. Mater. Sci. 18 (2000) 39.
[83] S.E. Collins, M.A. Baltanás, A.L. Bonivardi, unpublished results.
[84] O. Dulaurent, K. Chandes, C. Bouly, D. Bianchi, J. Catal. 188 (1999) 237.
[85] D.L. Chiavassa, A.L. Bonivardi, M.A. Baltanás, 13th International Congress on Catalysis, Paris, July 11–16 2004, to be presented.